Mesothelioma cells depend on the anti-apoptotic protein Bcl-xL for survival and are sensitized to ionizing radiation by BH3-mimetics

Mark R. Jackson[a], Miranda Ashton[a,b], Anna L. Koessinger[a,c], Craig Dick[b], Marcel Verheij[d], Anthony J. Chalmers[a,b,*]

[a] Institute of Cancer Sciences, University of Glasgow, Glasgow, UK

[b] Beatson West of Scotland Cancer Centre, Glasgow, UK

[c] Cancer Research UK Beatson Institute, Glasgow, UK

[d] Department of Radiation Oncology, Radboud University Medical Center, Nijmegen, The Netherlands

* Corresponding author: Prof. Anthony J Chalmers, Institute of Cancer Sciences, University of Glasgow, Glasgow G61 1QH, UK, e-mail: anthony.chalmers@glasgow.ac.uk

Running title: BH3-mimetics radiosensitize mesothelioma

Funding: This work was funded by the British Lung Foundation (MESO 15-13) and Beatson Cancer Charity (14-15-029)

Conflicts of interest: Anthony Chalmers has received honoraria from AbbVie Pharmaceuticals that are not related to the submitted work.

Acknowledgements: This work was funded by the British Lung Foundation and Beatson Cancer Charity. We thank Stephen Tait (University of Glasgow) for scientific advice and Kevin Blyth (Queen Elizabeth University Hospital, Glasgow) and Saurabh Dayal for isolation of primary MPM cells. Results include data generated by the TCGA Research Network: https://www.cancer.gov/tcga.

Keywords: mesothelioma, radiation, BH3-mimetic, Bcl-xL, radiosensitizer

Word count: 3728

Number of figures: 5

Number of tables: 0

ABSTRACT

The incidence of mesothelioma continues to rise and prognosis remains dismal due to resistance to conventional therapies and few novel treatment options. Failure to activate apoptotic cell death is a resistance mechanism that may be overcome by inhibition of anti-apoptotic Bcl-2 proteins using BH3-mimetic drugs. We investigated the role of anti-apoptotic proteins in the radioresistance of mesothelioma, identifying clinically-relevant targets for radiosensitization and evaluating the activity of BH3-mimetics alone and in combination with radiotherapy in pre-clinical models.

Mesothelioma cell lines 211H, H2052 and H226 exposed to BH3-mimetics demonstrated Bcl-xL dependence that correlated with protein expression and was confirmed by genetic knockdown. The Bcl-xL inhibitor A1331852 exhibited cytotoxic (EC_{50} 0.13-1.42 μmol/L) and radiosensitizing activities (sensitizer enhancement ratios 1.3-1.8). Cytotoxicity was associated with induction of mitochondrial outer membrane permeabilization and caspase-3/7 activation. Efficacy was maintained in a three-dimensional model in which combination therapy completely eradicated mesothelioma spheroids. Clinical applicability was confirmed by immunohistochemical analysis of Bcl-2 proteins in patient samples and radiosensitizing activity of A1331852 in primary patient-derived mesothelioma cells.

Mesothelioma cells exhibit addiction to the anti-apoptotic protein Bcl-xL and their intrinsic radioresistance can be overcome by small molecule inhibition of this novel therapeutic target.

INTRODUCTION

Malignant pleural mesothelioma (MPM) is an aggressive, asbestos-associated cancer with dismal outcome (median survival <10 months) (1). Curative treatment is currently prevented by intrinsic resistance to chemo- and radiotherapy, whereby the underlying mechanisms are poorly understood.

Ionizing radiation (IR) induces DNA damage that activates multiple stress pathways, including those mediated through p53. Unlike many cancers, p53 mutations are infrequent in MPM (2) perhaps because of the selective pressure imposed by asbestos-induced inflammation (1). This distinct disease aetiology likely necessitates development of mechanisms to resist death signals generated downstream of p53 activation.

Intrinsic apoptosis is initiated by inactivation of anti-apoptotic Bcl-2 proteins, which leads to mitochondrial outer membrane permeabilization (MOMP) and consequential cell death either through canonical caspase-dependent apoptosis or via caspase-independent mechanisms (3).

Bcl-2 proteins regulate apoptosis through interactions between pro- and anti-apoptotic partners (4), and the documented suppression of apoptosis in MPM cells by these proteins (5) identifies them as promising therapeutic targets in this disease (1,6). Small molecule mimetics of the pro-apoptotic BH3 domain antagonize anti-apoptotic Bcl-2 protein function, promoting cell death (7). Indeed the prototype pre-clinical BH3-mimetic ABT-737, which inhibits Bcl-2, Bcl-xL and Bcl-w, is active against MPM cells (8,9), and alternative strategies abrogating Bcl-2 protein function also induced apoptosis in MPM (9-12). Exploitation of the apoptotic priming exhibited by MPM cells, and their reliance on suppression of cell death pathways downstream of p53, creates a therapeutic opportunity for BH3-mimetics both as single agents and in combination with cytotoxic agents including IR (1,6,8). The recent development of novel

inhibitors with improved selectivity and enhanced pharmacokinetic properties creates an opportunity for targeting individual Bcl-2 proteins in the clinic (13).

Herein, we describe a specific role for Bcl-xL in the failure of MPM cells to execute apoptosis in response to IR, and demonstrate potent cytotoxic and radiosensitizing activities of the next-generation Bcl-xL inhibitor A1331852 in multiple MPM models.

MATERIALS & METHODS

Reagents

All reagents were purchased from Sigma-Aldrich, unless otherwise stated. Inhibitors of Bcl-2 proteins (A1155463, A1331852, ABT-199, ABT-263, UMI-77) were obtained from SelleckChem.

Cell culture

Mesothelioma cell lines MSTO-211H (211H) and NCI-H2052 (H2052) were provided by Sam Janes (University College London); NCI-H226 (H226) were supplied by John Lunec (University of Newcastle). Cells were maintained at 37 °C with 5% CO_2 in Advanced DMEM/F-12 medium supplemented with 10% FBS, L-glutamine (1 mmol/L), penicillin (50 units/mL) and streptomycin (50 µg/mL), and tested regularly for mycoplasma (Lonza). All experiments were performed within 10 passages of revival.

Transcriptomic analysis

RNAseq data were obtained from The Cancer Genome Atlas mesothelioma project (TCGA-MESO). The absence of normal tissue samples prohibited fold-change analysis, so relative gene expression was assessed using an approach similar to calculation of expression rank product (14). For each patient (*n*=86), normalized mapped reads (FPKM) were ranked for expression and assigned a rank product.

Immunohistochemistry

Formalin-fixed paraffin-embedded spheroid sections and clinical mesothelioma samples were subjected to antigen retrieval (Dako), blocked, and stained using antibodies to Ki67 (Dako #M724001-2, 1/100), active caspase-3 (Cell Signalling #9661, 1/500), Mcl-1 (Abcam #32087, 1/500), Bcl-2 (Leica # NCL-L-bcl-2, 1/200) and Bcl-xL (Abcam #ab32370, 1/300) overnight at 4 °C and HRP-conjugated secondary antibodies (Dako) at room temperature for 40 minutes. Staining was visualized using 3,3'-diaminobenzidine tetrahydrochloride (DAB, Dako); nuclei were counterstained with haematoxylin. Slides were digitally scanned and analysed using HALO software (PerkinElmer) to calculate an H-score for each sample based on the percentage of cells exhibiting mild, moderate or high staining intensity (ranging from 0 to 300).

Cell viability

Cell viability was assessed by CellTiterGlo (Promega) assay after 4 days of treatment. Cells were seeded overnight in 96-well plates and treated with inhibitors or vehicle control 4 hours prior to irradiation at room temperature (2 Gy). Irradiation was performed in a regularly calibrated X-ray cabinet (2.47 Gy/min, 195 kV, 15 mA, 0.5 mm Cu filter, X-Strahl). For caspase inhibition experiments, cells were pre-treated with QVD-OPh (QVD, Abcam) to a final concentration of 20 μmol/L for 1 hour, before exposure to A1331852 and IR (2 Gy). Cell viability was determined after 24 hours. Data were normalized to untreated controls or IR-only samples, and compared to controls by one-way ANOVA with post hoc Tukey test. Dose response parameters were obtained by fitting a 4-parameter dose response curve and were compared by F-test.

Western immunoblotting

Cells were treated with 5 Gy or sham irradiated, followed by a 24 hour incubation. Whole cell lysates were harvested before separation by SDS-PAGE, blotting, blocking, and probing with primary antibodies to β-tubulin (Abcam #ab21057, 1/1000), Bcl-xL (Abcam #ab32370,

1/1000), Mcl-1 (Abcam #ab32087, 1/1000), and Bcl-2 (Dako #M0887, 1/1000) overnight at 4 °C, and HRP-conjugated secondary antibodies (Cell Signalling Technology, 1/5000) for 1 hour at room temperature. Antibody binding was visualized using ECL reagent (Thermo Fisher Scientific) and imaged by LI-COR Odyssey Fc.

Knockdown of Bcl-xL expression

Cells were transfected using Lipofectamine RNAi Max (Thermo Fisher Scientific) with two independent siRNAs (Dharmacon); target sequences GGACAGCAUAUCAGAGCUU and CCUACAAGCUUUCCCAGAA. Mock transfection and non-targeting siRNA acted as controls. Lysates were harvested and assays performed 48 hours post-transfection.

Clonogenic survival assay

Cells were seeded at densities that generated >50 colonies per well and drug treated 4 hours pre-irradiation. After >7 days, colonies were washed, fixed in methanol, and stained with crystal violet. Surviving fraction (SF) was calculated using plating efficiencies (PE) of mock/vehicle-treated or drug only-treated cells. Data were fitted using the linear quadratic equation and curves compared using an exact sum-of-squares F-test. Sensitizer enhancement ratios were calculated using mean inactivation doses determined from the linear quadratic model. Differences between treatment groups were analysed by two-way ANOVA.

Immunofluorescence

Cells were seeded on glass coverslips overnight (10^4 cells/cm^2) before drug treatment and subsequent irradiation. Four hours later, cells were fixed, permeabilized, and blocked. Samples were immunostained using antibodies to Cytochrome C (BD Biosciences #556432, 1/500) and Bax (Cell Signalling Technology #2772, 1/500) for 1 hour at 37 °C and fluorophore-

conjugated secondary antibodies (Thermo Fisher Scientific, 1/500) for 1 hour at 37 °C. Nuclei were counterstained with DAPI (Dako). Five random fields-of-view were acquired using 20x/0.8 objective on a Zeiss LSM780 confocal microscope. The number of cells exhibiting punctate Bax and Cytochrome C release was manually counted and computed as the proportion of total cells for >50 cells/experiment, and normalized to vehicle control. Data were compared by one-way ANOVA with post hoc Tukey test. Example images were obtained using a 63x/1.4 objective.

Caspase-3/7 activity assay

Caspase-3/7 activity was quantified using a Caspase-Glo 3/7 assay (Promega). Cells were seeded overnight before 4 hour drug treatment and subsequent irradiation. Data were normalized to peak activity and compared by one-way ANOVA with post hoc Tukey test.

Spheroid growth

H2052 cells were seeded in ultra-low attachment plates (100 cells/well, Corning). After 4 days, spheroids were treated with inhibitor (3 μmol/L) or vehicle for 6 hours before exposure to 5 Gy. Brightfield imaging of spheroids was performed with a 5x/0.15 objective on a Zeiss Axio Vert.A1 microscope fitted with an AxioCam ICm1 camera, and volume estimated using Reconstruction and Visualization from a Single Projection (ReVISP) (15). Groups were compared at day 17 by one-way ANOVA with post hoc Tukey test.

Isolation of primary mesothelioma cells

Primary MPM cells were generated from surplus pleural fluid obtained during a therapeutic pleural aspiration under informed consent, cultured in conditions previously described for primary MPM cell lines (16) and used within two passages. Ethical approval for derivation and

use of primary MPM cells was provided by NHS Research Scotland Greater Glasgow & Clyde Biorepository (ref. 2014/175).

Statistical analysis

Statistical analyses were performed using R 3.5.0 (17) with the addition of the ‘drc’ package (18), as described for each experimental technique. Figures represent means±SD of 3 independent experiments, unless otherwise indicated.

RESULTS

Mesothelioma cells depend on Bcl-xL function for survival

Expression of Bcl-2 proteins in MPM was investigated using transcriptomic data within TCGA. Genes encoding Mcl-1 (MCL1), Bcl-2 (BCL2) and Bcl-xL (BCL2L1) were highly expressed in MPM, particularly MCL1 and BCL2L1 (Fig. 1A). Expression was consistent across all histological subtypes: epithelioid (57/86), biphasic (22/86), sarcomatoid (2/86) and diffuse malignant (5/86). High expression of both pro- and anti-apoptotic genes (Supplementary Fig. S1) supports the theory that MPM is primed for apoptotic death (8,19,20) and strengthens the rationale for targeting Bcl-2 proteins. High expression of genes encoding diagnostic markers of MPM (mesothelin, calbindin 2, keratin 5 and podoplanin) and low expression of exclusion markers (carcinoembryonic antigen related cell adhesion molecule 3; estrogen receptor 1) validated the samples studied and the expression ranking approach (21-23).

At the protein level, MPM samples exhibited low expression of active caspase-3 (Fig. 1B-C), indicating inhibition of apoptosis, and robust staining for at least one major anti-apoptotic Bcl-2 protein. Consistent with transcriptomic data, Mcl-1 and Bcl-xL levels were generally higher than Bcl-2, although some samples (e.g. patient 17) preferentially expressed Bcl-2.

Functional roles of Bcl-2 proteins were investigated using a panel of cell lines representing epithelioid (H226), sarcomatoid (H2052) and biphasic (211H) MPM subtypes. Expression of Mcl-1, Bcl-2 and Bcl-xL varied, with 211H cells exhibiting robust expression of all three proteins, H2052 expressing primarily Bcl-xL, and H226 exhibiting intermediate Mcl-1 and low Bcl-2 and Bcl-xL expression (Fig. 2A). Protein expression was unaltered by exposure to IR (5 Gy). Hence, different MPM tumours exhibit different patterns of Bcl-2 protein expression, which might confer differential dependencies on particular anti-apoptotic protein function. These dependencies were investigated using chemical BH3-profiling (24,25). Viability assays of MPM cells treated with BH3-mimetic inhibitors specific to Mcl-1 (UMI-77), Bcl-2 (ABT-199)

and Bcl-xL (A1155463) showed that Mcl-1 inhibition had minimal effect, while Bcl-2 inhibition had modest activity in 211H cells and minimal activity in the other cell lines (Fig. 2B). In contrast, Bcl-xL inhibition markedly reduced viability of 211H and H2052 cells (relative viabilities 0.28 and 0.27 at 1 μmol/L, respectively) and had modest activity against H226 cells (relative viability 0.18 at 10 μmol/L). Comparison with immunoblot data revealed a broad association between sensitivity to BH3-mimetics and Bcl-2 protein expression.

Survival dependency on Bcl-xL was corroborated by knockdown of expression using two independent siRNA constructs. Downregulation, confirmed by immunoblot (Fig. 2C), was associated with significant reductions in cell viability in all three cell lines (Fig. 2D).

Bcl-xL inhibition reduces mesothelioma cell survival through activation of MOMP

Having identified Bcl-xL as the most promising target, a second-generation inhibitor with improved potency and oral bioavailability (13), A1331852, was selected for further studies. A1331852 exhibited submicromolar potency against cells with high Bcl-xL expression, (EC_{50} values 0.270 μmol/L (95% confidence interval (CI) 0.139-0.400) and 0.133 μmol/L (95% CI 0.110-0.156) in 211H and H2052 cells respectively, Fig. 3A). Modest potency in H226 cells (EC_{50} 1.415 μmol/L, 95% CI 0.590-2.240) was consistent with lower Bcl-xL expression.

Ionizing radiation (IR, X-rays) induces apoptosis via the intrinsic pathway, and radioresistance of cancer cells is frequently associated with loss of this response. We hypothesized that combining Bcl-xL inhibition with IR would enhance efficacy and assessed this by measuring cell viability. Radiation alone (2 Gy) induced only a modest reduction in viability (Supplementary Fig. S2) but a therapeutic interaction with A1331852 was indicated by a significant reduction in drug EC_{50} in 211H (EC_{50} 0.032 μmol/L, 95% CI 0.016-0.048) and H2052 (0.031 μmol/L, 95% CI 0.025-0.036) cells (Fig. 3A). In H226 cells, an effect was detectable but failed to reach statistical significance (EC_{50} 0.502 μmol/L, 95% CI 0.191-0.813).

To investigate the specificity of these effects and understand the mechanisms involved, effects of A1331852 on apoptosis were determined at early time-points. We measured cellular MOMP 8 hours after treatment with A1331852 +/- IR (Fig. 3B, Supplementary Fig. S3). While IR alone (2 Gy) failed to induce MOMP (Fig. 3C), treatment with approximately isotoxic concentrations of A1331852 (viability ~40%; 1 µmol/L, 0.3 µmol/L and 3 µmol/L for 211H, H2052 and H226 respectively) robustly induced MOMP in 211H and H2052 cells. Maximal induction of MOMP was achieved in all cell lines by combining A1331852 with IR (2 Gy): 15.1, 11.9, and 4.9 fold increases in MOMP were observed in 211H, H2052, and H226 cells respectively.

Consistent with these observations, IR alone failed to increase caspase-3/7 activity, whereas A1331852 caused a marked increase in all three cell lines (Fig. 3D) and combination treatment further enhanced caspase-3/7 activation in cells expressing higher levels of Bcl-xL (211H and H2052), but not H226 cells.

The caspase-dependency (26,27) of A1331852-mediated death was next investigated using a broad-spectrum caspase inhibitor (QVD) in a 24 hour experiment, during which time canonical apoptosis is active. A1331852 reduced viability of MPM cells within 24 hours (Fig. 3E), whereas IR alone had no impact; and no combination-effects were apparent in this short-term assay. In H2052 and H226 cells, pre-treatment with the caspase inhibitor QVD partially protected cells against A1331852-mediated loss of viability, both with and without IR, indicating caspase-dependent apoptosis as the primary mechanism of cell death. In 211H cells, however, A1331852 reduced viability much less effectively over 24 hours than in longer term assays (e.g. Fig. 3A), implicating an alternative pathway of death in this cell line. Supporting this, and despite apparent activation of caspase-3/7 (Fig. 3D), QVD failed to protect 211H cells against A1331852-induced cell death (Fig. 3E), suggesting a MOMP-activated but caspase-independent mechanism of death, as previously described (27).

These findings indicate that the single agent and radiosensitizing activities of A1331852 are mediated through induction of MOMP, and that cell death proceeds via caspase-dependent apoptosis or in a caspase-independent manner depending on the cell line. Rapid activation of

MOMP after exposure to A1331852 supports our hypothesis that MPM cells are primed for mitochondrial cell death, which is otherwise suppressed by Bcl-xL.

Bcl-xL inhibition sensitizes mesothelioma cells to ionizing radiation

The radiosensitizing effects of A1331852 were validated by clonogenic survival, the gold standard measure of sensitivity to IR. IR alone caused modest reductions in clonogenicity, (SF_{4Gy} values 0.105, 0.156 and 0.184 for 211H, H2052 and H226 cells, respectively, Fig. 4A). To assess radiosensitization, cells were pre-incubated with A1331852 at concentrations that activated MOMP (Fig. 3C). Single agent activity of A1331852 was confirmed by reduced plating efficiency in H2052 and H226 cells (Supplementary Fig. S4A) and A1331852 significantly increased radiosensitivity, reducing SF_{4Gy} values to 0.032, 0.035, 0.095 for 211H, H2052, and H226, respectively (Fig. 4A). Formal quantification revealed clinically meaningful sensitizer enhancement ratios (SER) of 1.55, 1.80 and 1.30 in 211H, H2052 and H226 cells respectively.

To confirm the specificity of this effect and identify other candidates for clinical development, alternative Bcl-xL inhibitors were evaluated. Despite exhibiting lower single agent activity, the Bcl-xL-specific tool compound A1155463 and the Bcl-xL, Bcl-2 and Bcl-w inhibitor ABT-263 radiosensitized MPM cells with high Bcl-xL expression, but failed to overcome radioresistance in H226 cells (Supplementary Fig. S4A-D). Finally, siRNA knockdown of Bcl-xL reduced colony formation (Supplementary Fig. S4E) and effectively sensitized all three MPM cell lines to IR (Fig. 4B).

These findings indicate that chemical inhibition of Bcl-xL has potential as single agent and radiosensitizing therapy for MPM, and identify the clinically translatable compound A1331852 as the most promising agent in this class.

Bcl-xL inhibition shows efficacy against mesothelioma spheroids and patient-derived cells

Despite multiple attempts, we were unable to generate xenograft models of MPM that could support experiments evaluating radiotherapy-drug combinations. We therefore validated the therapeutic potential of A1331852 in MPM spheroids generated from H2052 cells, which resemble those observed in the pleural effusions of patients (28,29). This model expressed Bcl-xL and recapitulated clinical features including peripheral Ki67-positive proliferative cells and low baseline caspase-3 activation (Supplementary Fig. S5).

Spheroids treated with vehicle alone grew to an average volume of 0.341 mm^3 over 17 days (Fig. 5A). Single agent treatment with either IR (5 Gy) or A1331852 (3 µmol/L) caused measurable but temporary growth delay (volumes 0.158 and 0.074 mm^3 respectively, on day 17). In contrast, combination treatment caused complete and permanent regression such that spheroids were undetectable by day 12.

For further validation, tumour cells were isolated from the pleural effusion of a patient with epithelioid MPM (16) and treated with the radiotherapy-drug combination. In a single experiment, irradiation (2 Gy, Supplementary Fig. S6) and single agent treatment with A1331852 had modest effects on viability (EC_{50} 2.894 µmol/L, 95% CI 1.106-4.681) (Fig. 5B) but a striking therapeutic interaction between drug and IR was observed (EC_{50} 0.153 µmol/L, 95% CI 0.052 to 0.254), supporting the clinical applicability of this novel combination.

DISCUSSION

This pre-clinical study demonstrates the therapeutic potential of novel BH3-mimetics in MPM, both as single agents and radiosensitizers. Targeting Bcl-xL has been shown to sensitize MPM cells to different classes of chemotherapy (8,10,12,30), and the radiosensitizing potential of broad-spectrum BH3-mimetics such as ABT-737 has been demonstrated in other malignancies (31-33). We show for the first time that the Bcl-xL inhibitor A1331852 promotes MOMP in response to IR, leading to potent radiosensitization of primary and established MPM cells representing all histological disease subtypes. Combination efficacy was confirmed in a multicellular 3D model of MPM, a disease in which the presence of cell aggregates in pleural fluid correlates with disease malignancy (28). Since expression of Bcl-2 proteins is influenced by culture dimensionality (34), efficacy in 3D culture is a critical step in preclinical validation.

Clinical studies of BH3-mimetics have indicated 'on-target' haematological toxicity to be dose-limiting (35,36). The radiosensitizing activity of Bcl-xL inhibition raises the possibility of shortened treatments at lower drug concentrations, which may mitigate bone marrow suppression. In contrast to systemic chemotherapy (13), targeted thoracic radiotherapy is unlikely to exacerbate the haematological toxicity of Bcl-xL inhibition.

Genomic analysis of MPM samples has revealed a paucity of oncogenic mutations suitable for therapeutic targeting (2), supporting the adoption of broader, combinatorial strategies (1), such as reported here. These considerations, and the scarcity of representative experimental models of MPM, have contributed to neglect of this industrial disease of unmet need. By demonstrating dependency on Bcl-xL, our work identifies an important mechanism of therapy resistance and identifies a promising therapeutic strategy involving modulation of the apoptotic threshold in MPM cells.

REFERENCES

1. Blyth KG, Murphy DJ. Progress and challenges in Mesothelioma: From bench to bedside. *Respir Med* 2018;134:31-41.
2. Bueno R, Stawiski EW, Goldstein LD, et al. Comprehensive genomic analysis of malignant pleural mesothelioma identifies recurrent mutations, gene fusions and splicing alterations. *Nat Genet* 2016;48:407-16.
3. Giampazolias E, Zunino B, Dhayade S, et al. Mitochondrial permeabilization engages NF-kappaB-dependent anti-tumour activity under caspase deficiency. *Nat Cell Biol* 2017;19:1116-1129.
4. Kale J, Osterlund EJ, Andrews DW. BCL-2 family proteins: changing partners in the dance towards death. *Cell Death Differ* 2018;25:65-80.
5. Mohiuddin I, Cao X, Fang B, et al. Significant augmentation of pro-apoptotic gene therapy by pharmacologic bcl-xl down-regulation in mesothelioma. *Cancer Gene Ther* 2001;8:547-54.
6. Fennell DA, Rudd RM. Defective core-apoptosis signalling in diffuse malignant pleural mesothelioma: opportunities for effective drug development. *Lancet Oncol* 2004;5:354-62.
7. Rooswinkel RW, van de Kooij B, de Vries E, et al. Antiapoptotic potency of Bcl-2 proteins primarily relies on their stability, not binding selectivity. *Blood* 2014;123:2806-2815.
8. Barbone D, Ryan JA, Kolhatkar N, et al. The Bcl-2 repertoire of mesothelioma spheroids underlies acquired apoptotic multicellular resistance. *Cell Death Dis* 2011;2:e174.
9. Cao X, Yap JL, Newell-Rogers MK, et al. The novel BH3 alpha-helix mimetic JY-1-106 induces apoptosis in a subset of cancer cells (lung cancer, colon cancer and mesothelioma) by disrupting Bcl-xL and Mcl-1 protein-protein interactions with Bak. *Mol Cancer* 2013;12:42.
10. Cao X, Rodarte C, Zhang L, et al. Bcl2/bcl-xL inhibitor engenders apoptosis and increases chemosensitivity in mesothelioma. *Cancer Biol Ther* 2007;6:246-52.
11. Cao XX, Mohuiddin I, Ece F, et al. Histone deacetylase inhibitor downregulation of bcl-xl gene expression leads to apoptotic cell death in mesothelioma. *Am J Respir Cell Mol Biol* 2001;25:562-8.
12. Hopkins-Donaldson S, Cathomas R, Simoes-Wust AP, et al. Induction of apoptosis and chemosensitization of mesothelioma cells by Bcl-2 and Bcl-xL antisense treatment. *Int J Cancer* 2003;106:160-6.
13. Leverson JD, Phillips DC, Mitten MJ, et al. Exploiting selective BCL-2 family inhibitors to dissect cell survival dependencies and define improved strategies for cancer therapy. *Sci Transl Med* 2015;7:279ra40.
14. Breitling R, Armengaud P, Amtmann A, et al. Rank products: a simple, yet powerful, new method to detect differentially regulated genes in replicated microarray experiments. *FEBS Lett* 2004;573:83-92.
15. Piccinini F, Tesei A, Arienti C, et al. Cancer multicellular spheroids: volume assessment from a single 2D projection. *Comput Methods Programs Biomed* 2015;118:95-106.
16. Philippeaux MM, Pache JC, Dahoun S, et al. Establishment of permanent cell lines purified from human mesothelioma: morphological aspects, new marker expression and karyotypic analysis. *Histochem Cell Biol* 2004;122:249-60.
17. R Core Team. 2018; R: A language and environment for statistical computing. R Foundation for Statistical Computing, Vienna, Austria; URL https://www.R-project.org/.
18. Ritz C, Baty F, Streibig JC, et al. Dose-Response Analysis Using R. *Plos One* 2015;10.
19. Inoue-Yamauchi A, Jeng PS, Kim K, et al. Targeting the differential addiction to anti-apoptotic BCL-2 family for cancer therapy. *Nat Commun* 2017;8:16078.
20. Lopez J, Bessou M, Riley JS, et al. Mito-priming as a method to engineer Bcl-2 addiction. *Nat Commun* 2016;7.

21. Chernova T, Sun XM, Powley IR, et al. Molecular profiling reveals primary mesothelioma cell lines recapitulate human disease. *Cell Death Differ* 2016;23:1152-64.
22. Chirieac LR, Pinkus GS, Pinkus JL, et al. The immunohistochemical characterization of sarcomatoid malignant mesothelioma of the pleura. *Am J Cancer Res* 2011;1:14-24.
23. Shield PW, Koivurinne K. The value of calretinin and cytokeratin 5/6 as markers for mesothelioma in cell block preparations of serous effusions. *Cytopathology* 2008;19:218-223.
24. Butterworth M, Pettitt A, Varadarajan S, et al. BH3 profiling and a toolkit of BH3-mimetic drugs predict anti-apoptotic dependence of cancer cells. *Br J Cancer* 2016;114:638-41.
25. Peperzak V, Slinger E, Ter Burg J, et al. Functional disparities among BCL-2 members in tonsillar and leukemic B-cell subsets assessed by BH3-mimetic profiling. *Cell Death Differ* 2017;24:111-119.
26. Ekert PG, Read SH, Silke J, et al. Apaf-1 and caspase-9 accelerate apoptosis, but do not determine whether factor-deprived or drug-treated cells die. *J Cell Biol* 2004;165:835-842.
27. Lartigue L, Kushnareva Y, Seong Y, et al. Caspase-independent mitochondrial cell death results from loss of respiration, not cytotoxic protein release. *Mol Biol Cell* 2009;20:4871-4884.
28. Daubriac J, Fleury-Feith J, Kheuang L, et al. Malignant pleural mesothelioma cells resist anoikis as quiescent pluricellular aggregates. *Cell Death Differ* 2009;16:1146-1155.
29. Kim KU, Wilson SM, Abayasiriwardana KS, et al. A novel in vitro model of human mesothelioma for studying tumor biology and apoptotic resistance. *Am J Respir Cell Mol Biol* 2005;33:541-8.
30. Ozvaran MK, Cao XBX, Miller SD, et al. Antisense oligonucleotides directed at the bcl-xl gene product augment chemotherapy response in mesothelioma. *Mol Cancer Ther* 2004;3:545-550.
31. Li JY, Li YY, Jin W, et al. ABT-737 reverses the acquired radioresistance of breast cancer cells by targeting Bcl-2 and Bcl-xL. *J Exp Clin Cancer Res* 2012;31:102.
32. Wang H, Yang YB, Shen HM, et al. ABT-737 induces Bim expression via JNK signaling pathway and its effect on the radiation sensitivity of HeLa cells. *PLoS One* 2012;7:e52483.
33. Wu H, Schiff DS, Lin Y, et al. Ionizing radiation sensitizes breast cancer cells to Bcl-2 inhibitor, ABT-737, through regulating Mcl-1. *Radiat Res* 2014;182:618-625.
34. Xiang X, Phung Y, Feng M, et al. The development and characterization of a human mesothelioma in vitro 3D model to investigate immunotoxin therapy. *PLoS One* 2011;6:e14640.
35. Gandhi L, Camidge DR, Ribeiro de Oliveira M, et al. Phase I study of Navitoclax (ABT-263), a novel Bcl-2 family inhibitor, in patients with small-cell lung cancer and other solid tumors. *J Clin Oncol* 2011;29:909-16.
36. Rudin CM, Hann CL, Garon EB, et al. Phase II study of single-agent navitoclax (ABT-263) and biomarker correlates in patients with relapsed small cell lung cancer. *Clin Cancer Res* 2012;18:3163-9.

FIGURE LEGENDS

Figure 1. Bcl-2 proteins are highly expressed in clinical mesothelioma samples.

(A) Expression of MCL1, BCL2 and BCL2L1 genes determined across MPM subtypes from patient transcriptomic data (TCGA). Data were plotted for each patient (*n*=86), with median expression represented by lines. Rank product quartiles are indicated. (B) Clinical mesothelioma tumour sections stained for Ki67 and apoptotic proteins. Samples were counterstained with haematoxylin. (C) Automatic stain quantification represented by H-score. Box and whiskers were plotted according to the Tukey method (*n*=18).

Figure 2. Mesothelioma cells depend on Bcl-xL function for survival.

(A) Immunoblotting showing expression of Mcl-1, Bcl-2 and Bcl-xL proteins in MPM cells. Cells were treated with 5 Gy X-rays or sham irradiation and lysates harvested after 24 hours. (B) Relative viability of MPM cells treated with BH3-mimetics targeting Mcl-1, Bcl-2 and Bcl-xL measured 96 hours after treatment. (C) siRNA-mediated reduction in Bcl-xL expression assessed by immunoblotting at 48 hours. (D) Relative viability of cells transfected with siRNA constructs for 48 hours determined after 96 hours. Bars represent mean±SD of 3 independent experiments. Groups were compared by one-way ANOVA with post hoc Tukey test. *** $P<0.001$ compared to vehicle or mock transfected controls.

Figure 3. A1331852 activates apoptosis in response to IR in mesothelioma cells.

(A) Relative viability of MPM cells measured 96 hours after treatment with A1331852, alone or in combination with 2 Gy X-rays. Points represent mean±SD of 3 independent experiments; EC_{50} values were determined by fitting a 4-parameter dose response curve. (B) An example of the MOMP phenotype in H2052 cells assessed by immunofluorescent staining of Bax (green) and Cytochrome C (red), 8 hours after exposure to A1331852 and IR (2 Gy X-rays). Nuclei counterstained with DAPI (blue); scale bar 20 μm. (C) Quantification of fold induction of MOMP. (D) Activation of caspase-3/7 measured following 24 hour treatment with A1331852 and IR (2 Gy X-rays), normalized for peak activity. (E) Relative viability of cells treated with A1331852 and IR (2 Gy X-rays) assessed after 24 hours, with or without pre-treatment with the caspase inhibitor QVD. Bars represent mean±SD of 3 independent experiments and were compared by one-way ANOVA with post hoc Tukey test. *** or ### P<0.001, ** or ## P<0.01, * or # P<0.05 (* compared to 0 Gy DMSO, # comparison as indicated).

Figure 4. Bcl-xL inhibition sensitizes mesothelioma cells to ionizing radiation.

(A) Clonogenic survival of cells treated with IR (X-rays) alone or in combination with A1331852. (B) Clonogenic survival of cells treated with IR (X-rays) alone or in combination with siRNAs targeting Bcl-xL. Points represent mean±SD of 3 independent experiments, and were fitted using the linear quadratic model; curves were compared by F-test. *** P<0.001, ** P<0.01 compared to vehicle control (DMSO) or mock treated samples. Sensitizer enhancement ratios (SER) were calculated according to the mean inactivation dose method.

Figure 5. A1331852 exhibits efficacy in advanced pre-clinical models of mesothelioma.

(A) Growth of MPM spheroids treated with IR (5 Gy X-rays) and A1331852 (3 μmol/L) measured over 17 days. H2052 cells were grown as spheroids and treated at day 0. Points represent mean±SD of 3 independent experiments, compared by one-way ANOVA with post hoc Tukey test at day 17. ** $P<0.01$, * $P<0.05$, comparison as indicated. Scale bar 1 mm. (B) Relative viability of primary MPM cells measured 96 hours after treatment with A1331852, alone or in combination with 2 Gy X-rays. Points represent mean±SD of 2 technical replicates from a single experiment; EC_{50} values were determined by fitting a 4-parameter dose response curve.

Figure 1

A

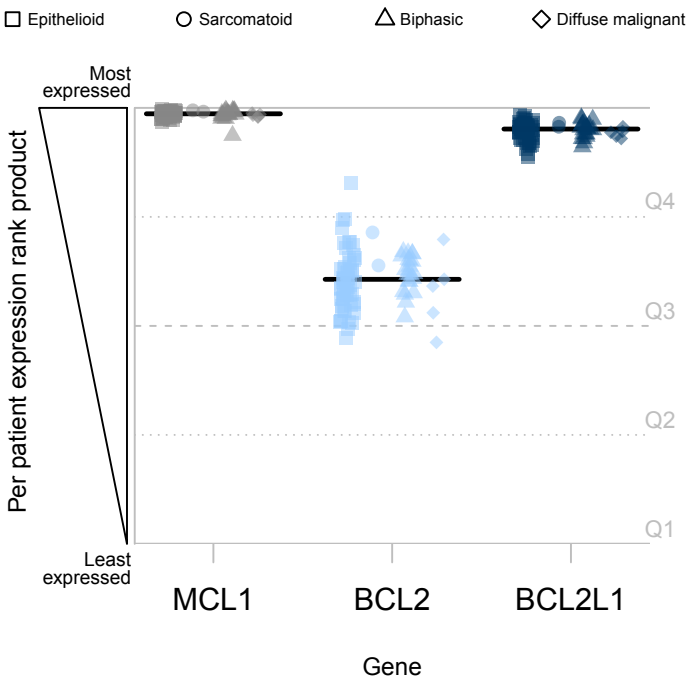
Epithelioid
Sarcomatoid
Biphasic
Diffuse malignant
Most expressed
Least expressed
Per patient expression rank product
Q4
Q3
Q2
Q1
MCL1
BCL2
BCL2L1
Gene

Figure 1 (continued)

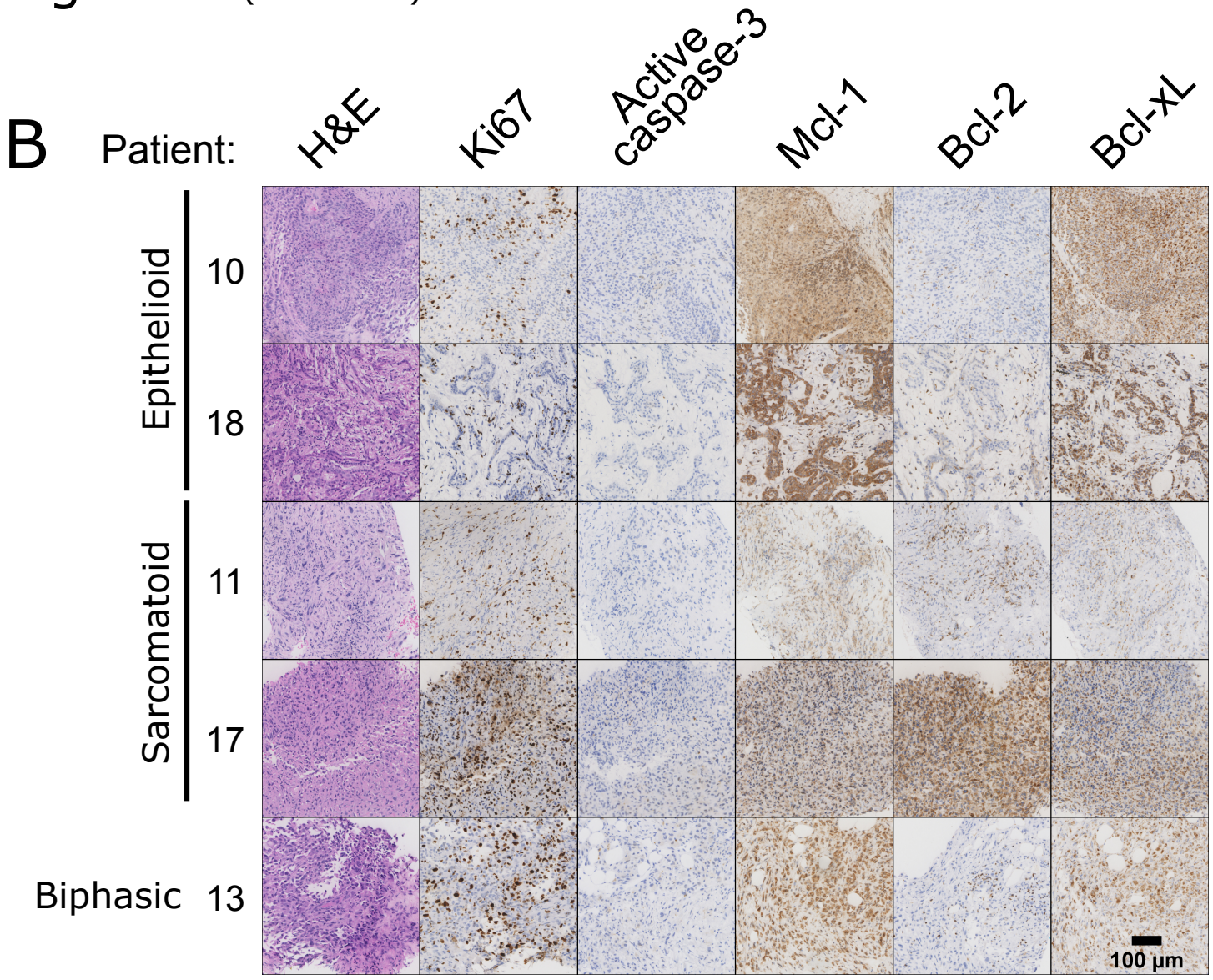

Figure 1 (continued)

C

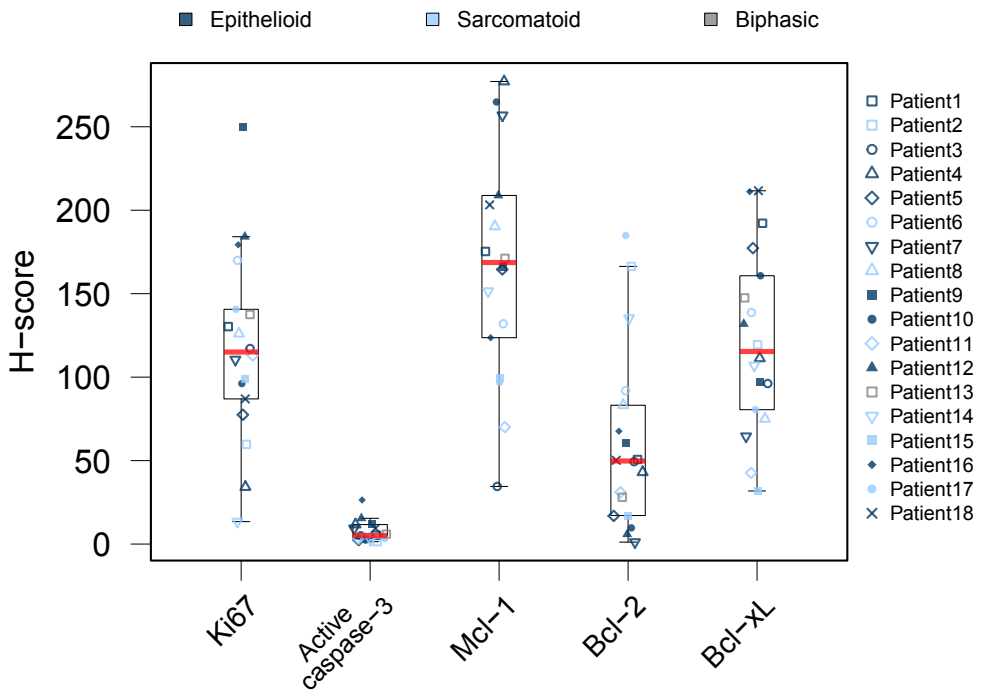

Figure 2

A

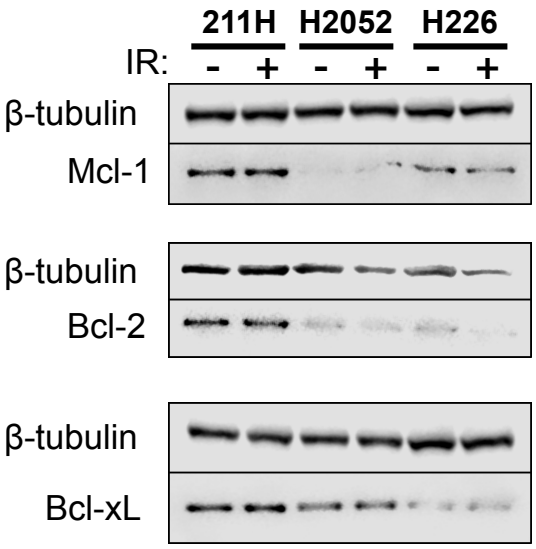
211H
H2052
H226
IR:
- + - + - +
β-tubulin
Mcl-1
β-tubulin
Bcl-2
β-tubulin
Bcl-xL

Figure 2 (continued)

B

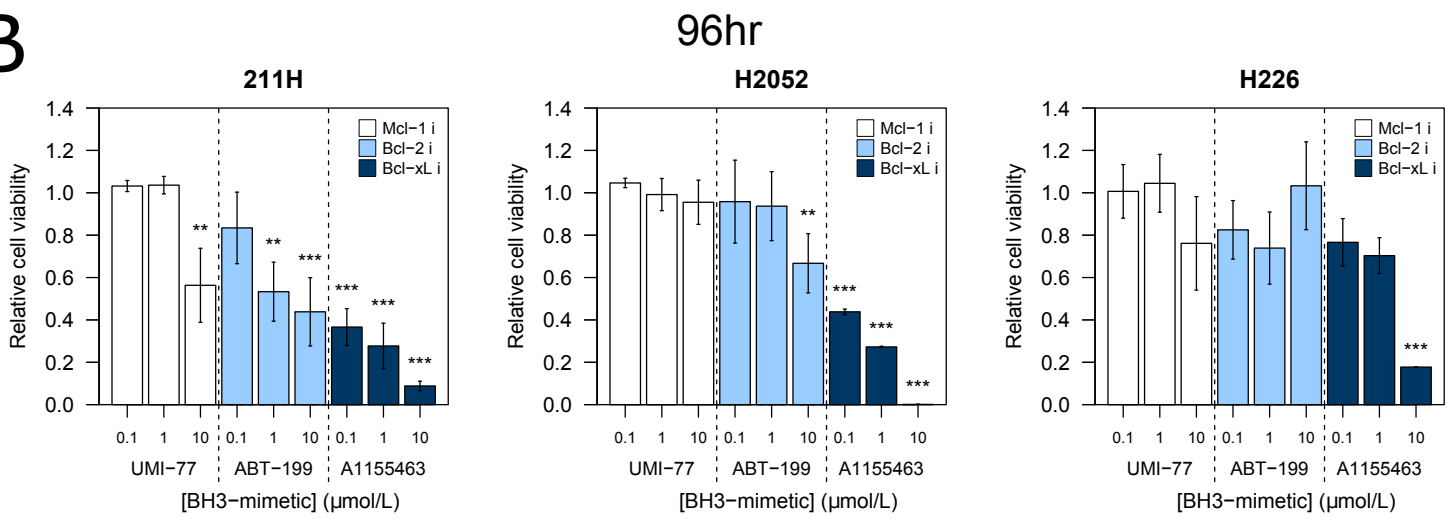

Figure 2 (continued)

C

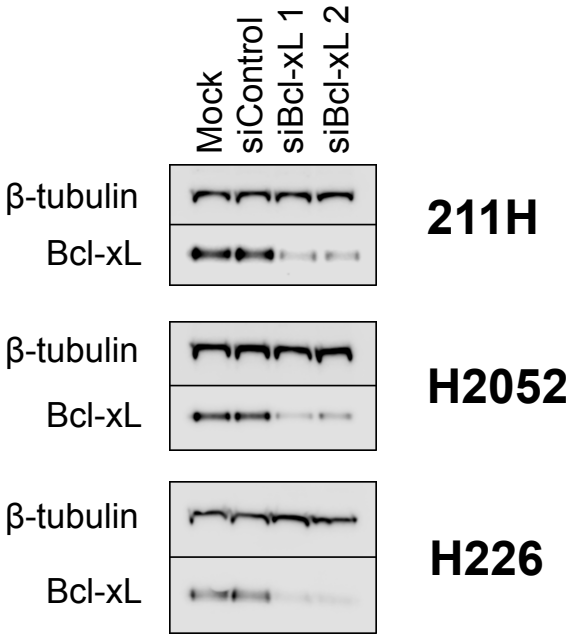

Figure 2 (continued)

D

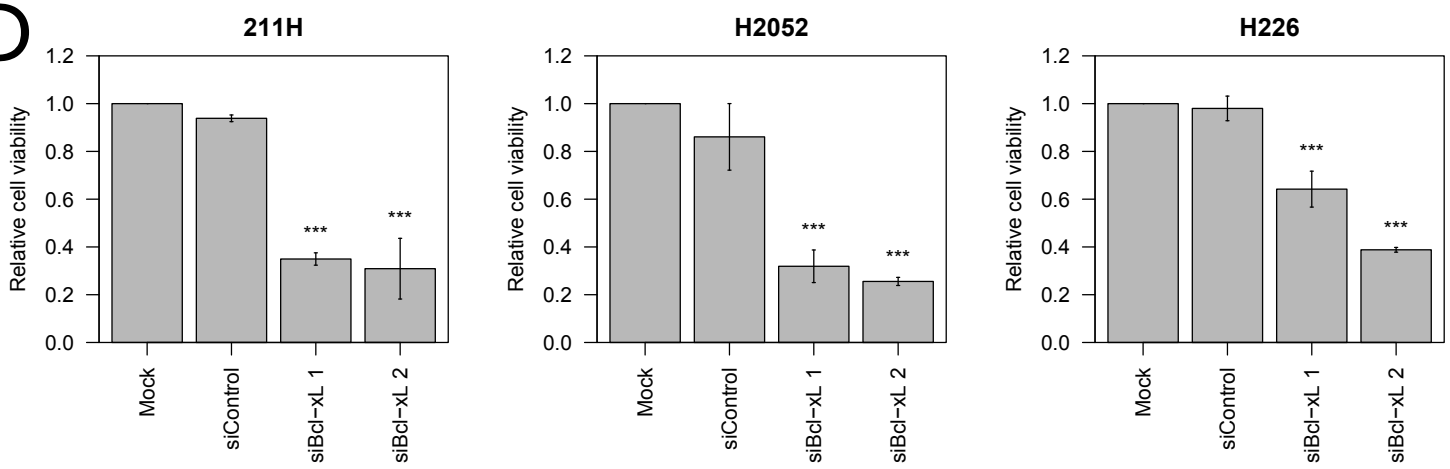

Figure 3

A

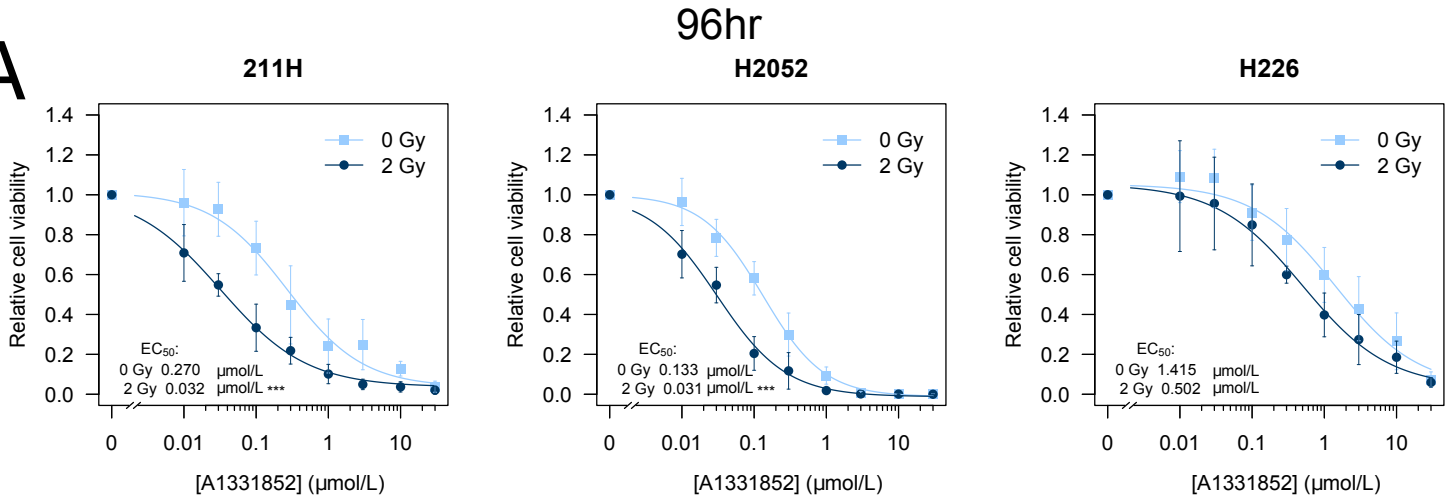
96hr
211H
H2052
H226
Relative cell viability
[A1331852] (µmol/L)
0 Gy
2 Gy
EC50:
0 Gy 0.270 µmol/L
2 Gy 0.032 µmol/L ***
0 Gy 0.133 µmol/L
2 Gy 0.031 µmol/L ***
0 Gy 1.415 µmol/L
2 Gy 0.502 µmol/L

Figure 3 (continued)

B

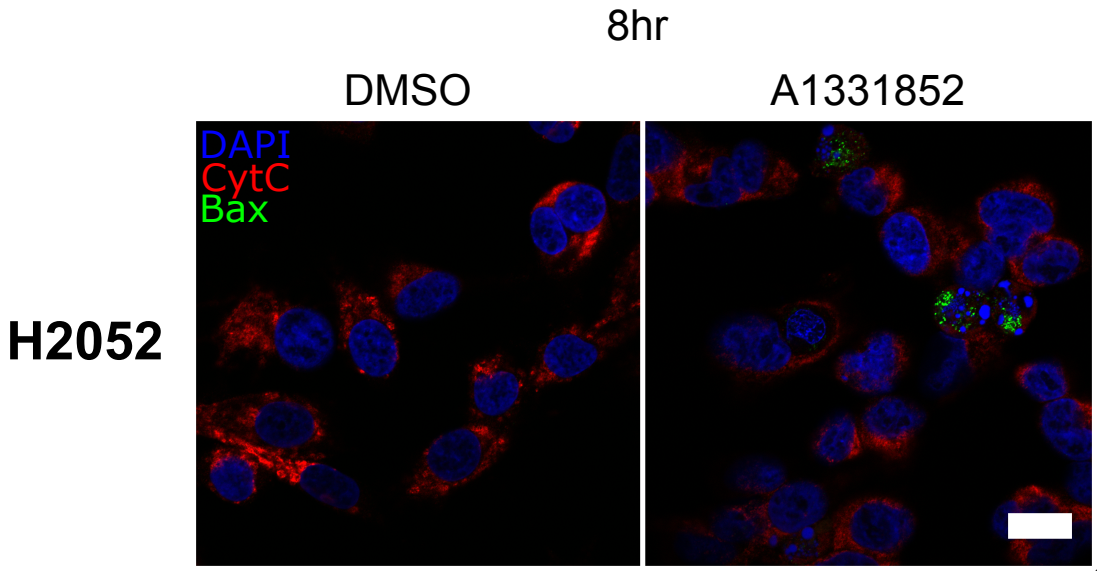

Figure 3 (continued)

C

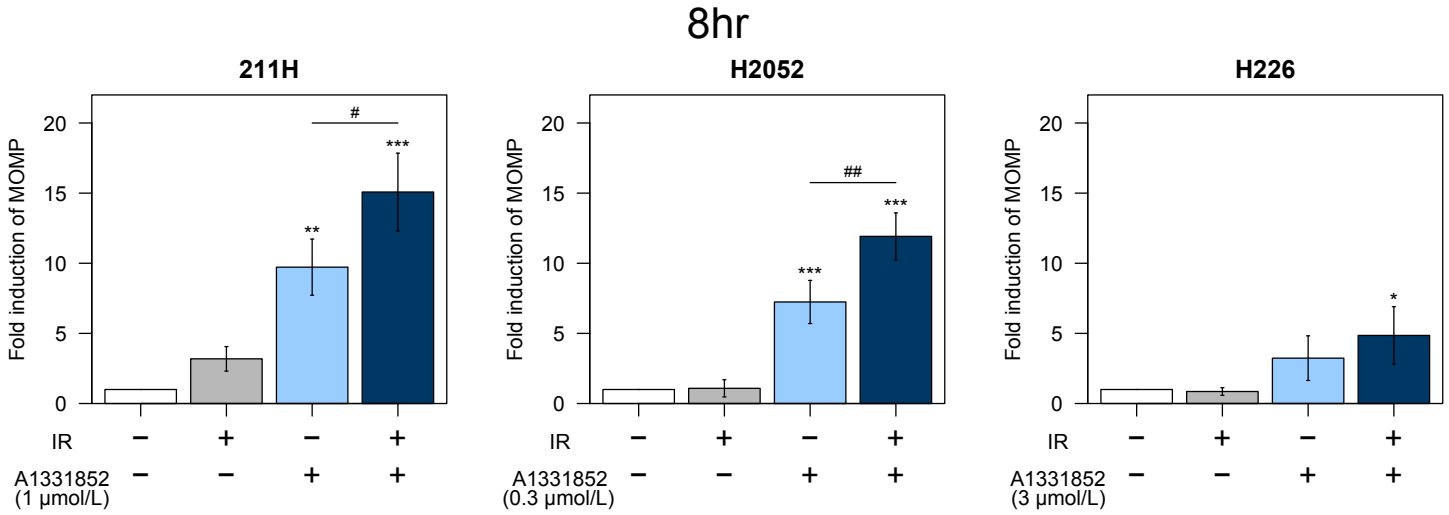

Figure 3 (continued)

D

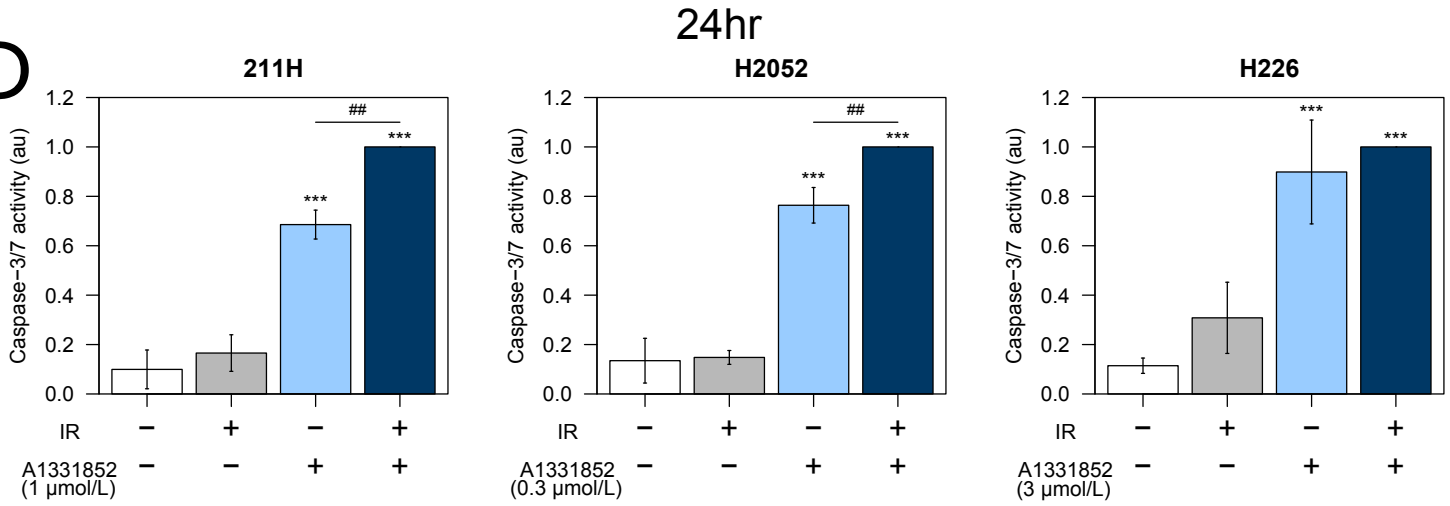

Figure 3 (continued)

E

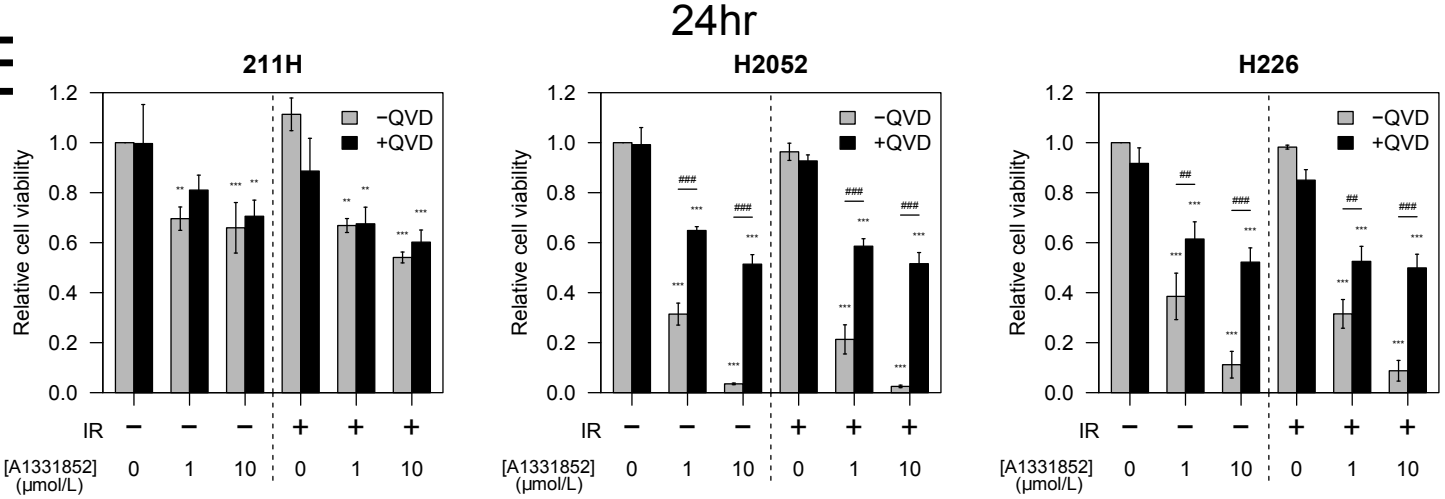

Figure 4

A

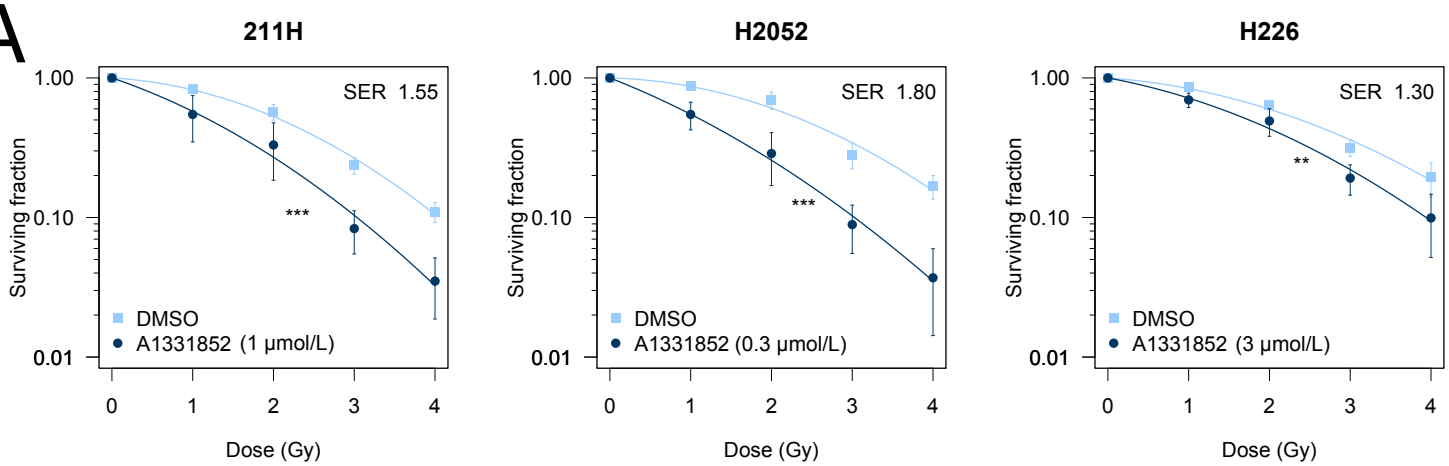
211H
H2052
H226
1.00
0.10
0.01
Surviving fraction
SER 1.55
SER 1.80
SER 1.30
***
***
**
DMSO
A1331852 (1 µmol/L)
A1331852 (0.3 µmol/L)
A1331852 (3 µmol/L)
0
1
2
3
4
Dose (Gy)

Figure 4 (continued)

B

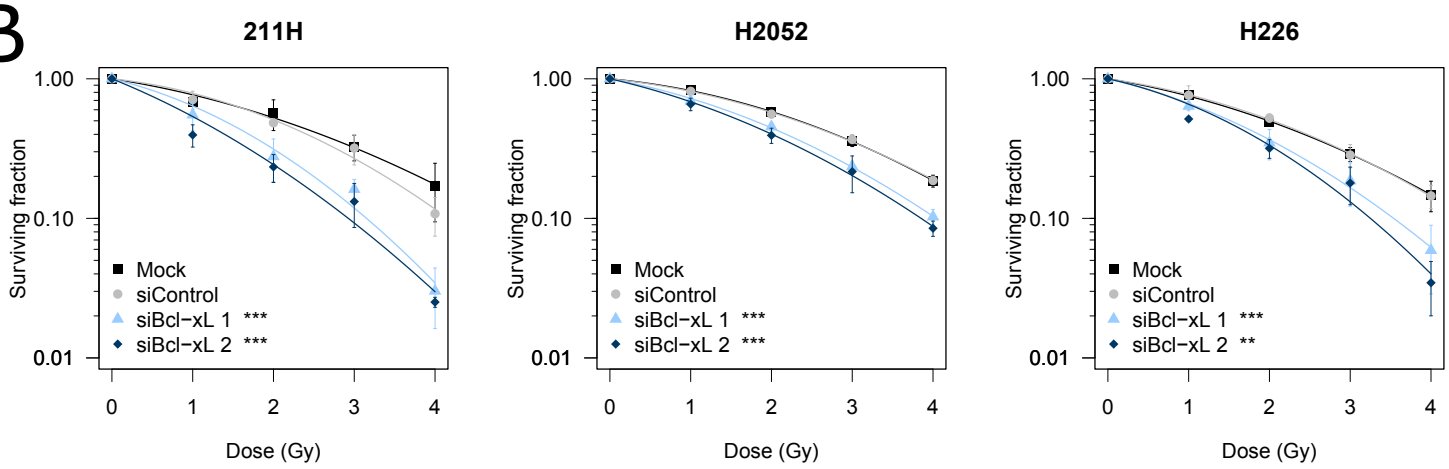

Figure 5

A

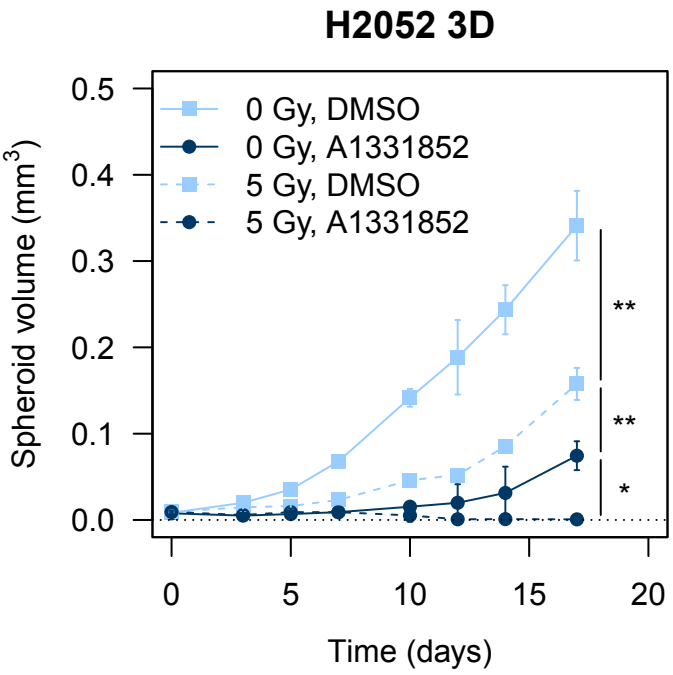
H2052 3D
0 Gy, DMSO
0 Gy, A1331852
5 Gy, DMSO
5 Gy, A1331852
Spheroid volume (mm3)
0.0
0.1
0.2
0.3
0.4
0.5
0
5
10
15
20
Time (days)
**
**
*

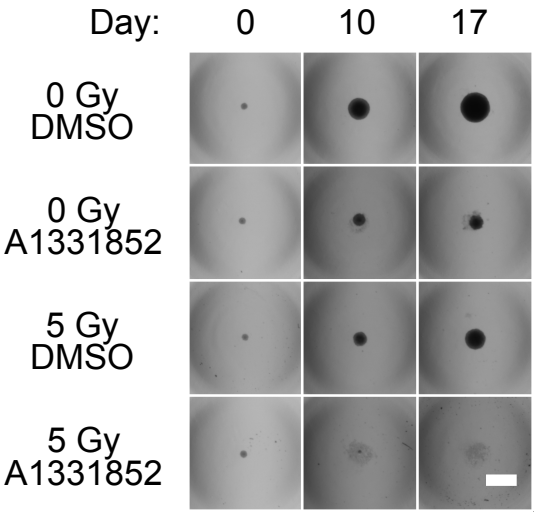
Day:
0
10
17
0 Gy DMSO
0 Gy A1331852
5 Gy DMSO
5 Gy A1331852

Figure 5 (continued)

B